Core-annular flow through a horizontal pipe: Hydrodynamic counterbalancing of buoyancy force on core

G. Ooms
J. M. Burgerscentrum, Faculty of Mechanical Engineering, Laboratory for Aero- and Hydrodynamics, Delft University of Technology, Mekelweg 2, 2628 CD Delft, The Netherlands

C. Vuik
J. M. Burgerscentrum, Faculty of Electrical Engineering, Mathematics and Computer Science, and Delft Institute of Applied Mathematics, Delft University of Technology, Mekelweg 4, 2628 CD Delft, The Netherlands

P. Poesio
Università di Brescia, Via Branze 38, 25123 Brescia, Italy

(Received 19 April 2007; accepted 19 July 2007; published online 28 September 2007)

A theoretical investigation has been made of core-annular flow: the flow of a high-viscosity liquid core surrounded by a low-viscosity liquid annular layer through a horizontal pipe. Special attention is paid to the question of how the buoyancy force on the core, caused by a density difference between the core and the annular layer, is counterbalanced. From earlier studies it is known that at the interface between the annular layer and the core waves are present that move with respect to the pipe wall. In the present study the core is assumed to consist of a solid center surrounded by a high-viscosity liquid layer. Using hydrodynamic lubrication theory (taking into account the flow in the low-viscosity liquid annular layer and in the high-viscosity liquid core layer) the development of the interfacial waves is calculated. They generate pressure variations in the core layer and annular layer that can cause a net force on the core. Steady eccentric core-annular flow is found to be possible. © *2007 American Institute of Physics*. [DOI: 10.1063/1.2775521]

I. INTRODUCTION

In transporting a high-viscosity liquid through a pipe a low-viscosity liquid can be used as a lubricant film between the pipe wall and the high-viscosity core. This technique, called core-annular flow, is very interesting from a practical and scientific point of view. In a number of cases it was successfully applied for pipeline transport of very viscous oil. The low-viscosity liquid in these cases was water. The pressure drop over the pipeline was considerably lower for oil-water core-annular flow than the pressure drop for the flow of oil alone at the same mean oil velocity.

Much attention has been paid in the literature to core-annular flow. Joseph and Renardi[1] have written a book about it. There are several review articles, see for instance, Oliemans and Ooms[2] and Joseph *et al.*[3] Most publications deal with the development of waves at the interface between the high-viscosity liquid and the low-viscosity one, see Ooms,[4] Bai *et al.*,[5] Bai *et al.*,[6] Renardy,[7] Li and Renardy,[8] Kouris and Tsamopoulos,[9] and Ko *et al.*[10] These studies deal with axisymmetric vertical core-annular flow (the core has a concentric position in the pipe). In that case the buoyancy force on the core, due to a density difference between the two liquids, is in the axial direction of the pipe. It was shown experimentally and theoretically that both liquid phases can retain their integrity, although an originally smooth interface was found to be unstable.

For the transport of very viscous oil (or other liquids) it is also important to pay attention to core-annular flow through a horizontal pipe. Since the densities of the two liquids are almost always different, gravity will push the core off-center in that case. Experimental results suggest that under normal conditions a steady eccentric core-annular flow (rather than a stratified flow) is achieved. It can be shown, that for a steady flow a wavy interface is needed to levitate the core. Relatively little attention has been given to the explanation of the levitation mechanism. Ooms,[11] Ooms and Beckers,[12] Ooms *et al.*,[13] Oliemans and Ooms,[2] and Oliemans[14] proposed a mechanism based on hydrodynamic lubrication theory. They showed that levitation could not take place without a hydrodynamic lifting action due to the waves present at the oil-water interface. They concluded from their experiments, that there are limitations to the parameter values that produce levitation. For instance, it became clear that the viscosity of the core liquid had to be much larger than the viscosity of the annular liquid. In their theoretical work they assumed that the core viscosity is infinitely large. So any deformation of the interface was neglected and the core moved as a rigid body at a certain speed with respect to the pipe wall. The shape of the waves was given as empirical input. They were assumed to be sawtooth waves, that were like an array of slipper bearings and pushed off the core from the wall by lubrication forces. In their case the core would be sucked to the pipe wall if the velocity was reversed. So the slipper bearing picture is obligatory if levitation is needed. However it was pointed out by Bai *et al.*,[6] that (at finite oil viscosity) the sawtooth waves are unstable since the pressure is highest just where the gap between the core and the pipe wall is smallest. So the wave must steepen

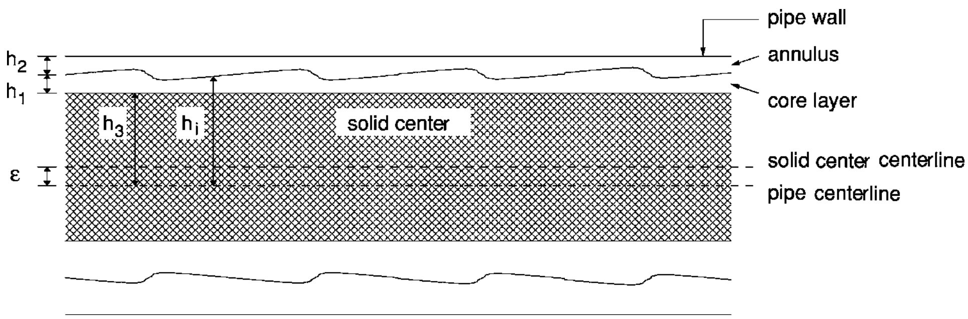

FIG. 1. Sketch of the flow problem.

where it is gentle and become smooth where it is sharp, and levitation of the core due to lubrication forces is no longer possible. To get a levitation force from this kind of wave inertial forces are needed according to Bai *et al.*

From their study of the wave development for a concentric vertical core-annular flow (taking into account inertial forces) Bai *et al.* tried to draw some conclusions about the levitation force on the core in the case of an eccentric horizontal core-annular flow. They considered what might happen if the core moved to a slightly eccentric position owing to a small difference in density. The pressure distribution in the liquid in the narrow part of the annulus would intensify and the pressure in the wide part of the annulus would relax according to their predicted variation of pressure with the distance between the core and the pipe wall for the concentric case. In that case a more positive pressure would be generated in the narrow part of the annulus which would levitate the core. (It is important to point out again that the study of Bai *et al.* was for a concentric core. In a horizontal core-annular flow with a density difference between the liquids the core will be in an eccentric position and due to the presence of waves at the interface secondary flows perpendicular to the pipe axis are generated. This type of secondary flows that also contribute to the force on the core, is not considered in concentric core-annular flow.)

The statement by Bai *et al.* that a levitation of the core does not come from lubrication forces but from inertial forces was made for cylindrically symmetric waves. The waves that were used in their calculation were periodic in the axial direction of the pipe and were independent of the circumferential coordinate. As found by Renardy[7] also waves are possible that are not cylindrically symmetric; waves that are dependent on the axial direction and also on the circumferential direction. It seems evident that for such waves the force on the core and also the secondary flow in the annulus will be different than for a core with cylindrically symmetric waves. Therefore Ooms and Poesio[15] studied the levitation of the core for the case of noncylindrically symmetric waves by investigating the hydrodynamic lubrication forces. They showed that core levitation by lubrication forces alone is possible for these types of waves. However, like in the earlier work of Ooms[11] and Oliemans[14] they assumed that the core viscosity is infinitely large. So the core (with waves) moves as a rigid body at a certain velocity with respect to the pipe wall.

Another contribution to the core levitation force was proposed in a model by Bannwarth.[16] It is based on an interface-curvature-gradient effect associated with interfacial tension; if the radius of curvature increases with the circumferential coordinate a downward force acts on the core due to interfacial tension.

In this publication a further development is made of the idea, that (eccentric) core-annular flow through a horizontal pipe with a density difference between the core liquid and the liquid in the annulus is possible due to hydrodynamic lubrication forces caused by the movement of waves at the core-annular interface with respect to the pipe wall. Contrary to earlier work the core is no longer assumed to be solid. The core is assumed to consist of a solid center surrounded by a high-viscosity liquid layer. (The problem in which the complete core has a finite viscosity cannot be solved by the authors by means of the partly analytical and partly numerical method that is applied in this publication.) Using hydrodynamic lubrication theory (taking into account the flow in the low-viscosity liquid annular layer and in the high-viscosity liquid core layer) the development of the interfacial waves will be calculated. Also the force exerted on the core will be determined, with special attention being paid to the position of the core with respect to the pipe wall.

Papageorgiou *et al.*,[17] Wei and Rumschitzki,[18] and others have all developed lubrication models for axisymmetric core-annular flow. They derive nonlinear evolution equations for the interface between the two liquids. These equations include a coupling between core and annular film dynamics thus enabling a study of its effect on the nonlinear evolution of the interface. A difference between their work and our study is, that we take into account the upward buoyancy force on the core (in a horizontal pipe) due to the density difference between the two liquids. Because of the buoyancy force we will also consider the eccentricity of the core, whereas Papageorgiou, Rumschitzki and others study axisymmetric core-annular flow.

II. THEORY

A sketch of the flow problem is given in Fig. 1. The pipe is horizontal. As mentioned the core is assumed to consist of a solid center surrounded by a high-viscosity liquid layer (the core layer). The solid center and core layer have the same density. The core (solid center and core layer) is surrounded by a low-viscosity liquid annular layer (the annulus). When the density of the core is smaller than the density of the annulus, the core has an eccentric position in the pipe. In that case the thickness of the annulus at the top of the pipe is smaller than its thickness at the bottom. In real core-annular flows the thickness of the annulus h_2 is small compared to the pipe radius R (smaller as shown in the figure). In the upcoming calculation we assume that also the thickness of the core layer h_1 is much smaller than the pipe radius. The (horizontal) solid center is cylindrically symmetric with known radius $h_3^{(0)}$. The distance between the center line of the pipe and the surface of the solid center is given by h_3. When the core has an eccentric position in the pipe, also the solid center is eccentric with the same eccentricity ϵ as the core. So when the eccentricity is known, also h_3 is known. The relation between h_1 and h_2 is given by $h_1 = R - h_3 - h_2$. A reference system is chosen according to which the solid center of the core is at rest and the pipe wall moves with a velocity w_w. At the interface between the core layer and the annulus waves are present, that move with respect to the pipe wall. The shape of the waves can depend on both the axial direction x and the circumferential direction θ. They are periodic. The liquid in the core layer (liquid 1) and the liquid in the annulus (liquid 2) are assumed to be incompressible. The liquids move in the axial and circumferential direction due to the movement of the waves and the (possible) eccentric position of the core in the pipe.

A. Pressure equation for the annulus

The order of magnitude of the terms in the continuity equation for the annulus are

$$\begin{array}{ccccc} \dfrac{1}{r}\dfrac{\partial}{\partial r}(ru_2) & + & \dfrac{1}{r}\dfrac{\partial v_2}{\partial \theta} & + & \dfrac{\partial w_2}{\partial x} = 0 \\ O\left(\dfrac{U_2}{h_2}\right) & & O\left(\dfrac{V_2}{R}\right) & & O\left(\dfrac{W_2}{l}\right), \end{array} \tag{1}$$

in which r, θ, and x are the cylindrical coordinates in the radial, circumferential, and axial direction, respectively. $\theta = 0$ at the top of the pipe and increases in the clockwise direction. u_2, v_2, and w_2 are the velocity components of the liquid in the annulus in the radial, circumferential, and axial direction and U_2, V_2, and W_2 are the velocity scales for u_2, v_2, and w_2. This means that

$$U_2 \ll V_2 \sim W_2 \tag{2}$$

when

$$h_2 \ll R \sim l. \tag{3}$$

The time scales in the r-direction (h_2/U_2), in the θ-direction (R/V_2) and in the x-direction (l/W_2) are of the same order of magnitude.

To estimate the order of magnitude of the terms in the equations of motion for the annulus it is first assumed that the Reynolds number of the flow is so small that the inertial terms may be neglected. So both the time-derivative terms and the convective terms in the equations of motion will be neglected in our model. The time dependency of the flow will be taken into account by means of the kinematic boundary condition, as will be explained later. The flow is laminar. The order of magnitude of the remaining terms in the equations of motion are given by

$$\begin{array}{ccccccc} \dfrac{1}{\eta_2}\dfrac{\partial \phi_2}{\partial r} = \dfrac{\partial}{\partial r}\left\{\dfrac{1}{r}\dfrac{\partial}{\partial r}(u_2 r)\right\} & + & \dfrac{1}{r^2}\dfrac{\partial^2 u_2}{\partial \theta^2} & + & \dfrac{\partial^2 u_2}{\partial x^2} & - & \dfrac{2}{r^2}\dfrac{\partial v_2}{\partial \theta} \\ O\left(\dfrac{U_2}{h_2^2}\right) & & O\left(\dfrac{U_2}{R^2}\right) & & O\left(\dfrac{U_2}{l^2}\right) & & O\left(\dfrac{V_2}{R^2}\right), \end{array} \tag{4}$$

$$\begin{array}{ccccccc} \dfrac{1}{\eta_2 r}\dfrac{\partial \phi_2}{\partial \theta} = \dfrac{\partial}{\partial r}\left\{\dfrac{1}{r}\dfrac{\partial}{\partial r}(v_2 r)\right\} & + & \dfrac{1}{r^2}\dfrac{\partial^2 v_2}{\partial \theta^2} & + & \dfrac{\partial^2 v_2}{\partial x^2} & + & \dfrac{2}{r^2}\dfrac{\partial u_2}{\partial \theta} \\ O\left(\dfrac{V_2}{h_2^2}\right) & & O\left(\dfrac{V_2}{R^2}\right) & & O\left(\dfrac{V_2}{l^2}\right) & & O\left(\dfrac{U_2}{R^2}\right), \end{array} \tag{5}$$

$$\begin{array}{ccccc} \dfrac{1}{\eta_2}\dfrac{\partial \phi_2}{\partial x} = \left\{\dfrac{1}{r}\dfrac{\partial}{\partial r}\left(r\dfrac{\partial w_2}{\partial r}\right)\right\} & + & \dfrac{1}{r^2}\dfrac{\partial^2 w_2}{\partial \theta^2} & + & \dfrac{\partial^2 w_2}{\partial x^2} \\ O\left(\dfrac{W_2}{h_2^2}\right) & & O\left(\dfrac{W_2}{R^2}\right) & & O\left(\dfrac{W_2}{l^2}\right), \end{array} \tag{6}$$

in which

$$\phi_2 = p_2 + \rho_2 g r \cos\theta, \tag{7}$$

where p_2 represents the hydrodynamic pressure in the annulus, ρ_2 is the density of the liquid in the annulus and g is the acceleration due to gravity. η_2 is the dynamic viscosity of the liquid. Using Eqs. (2) and (3), Eqs. (4)–(6) can be simplified by keeping only the largest terms in the set of equations (not in each equation separately). This leads to

$$\frac{\partial \phi_2}{\partial r} = 0, \tag{8}$$

$$\frac{1}{r}\frac{\partial \phi_2}{\partial \theta} = \eta_2 \frac{\partial}{\partial r}\left\{\frac{1}{r}\frac{\partial}{\partial r}(v_2 r)\right\}, \tag{9}$$

$$\frac{\partial \phi_2}{\partial x} = \left\{\frac{\eta_2}{r}\frac{\partial}{\partial r}\left(r\frac{\partial w_2}{\partial r}\right)\right\}. \tag{10}$$

So in this approximation ϕ_2 is independent of r, and the r-dependence of p_2 is given by Eq. (7). Integration of Eqs. (9) and (10) in the r-direction gives

$$v_2 = \frac{1}{2\eta_2}\frac{\partial \phi_2}{\partial \theta} r\left(-\frac{1}{2} + \ln r\right) + K_1 r + \frac{K_2}{r}, \tag{11}$$

$$w_2 = \frac{1}{4\eta_2}\frac{\partial \phi_2}{\partial x} r^2 + K_3 \ln r + K_4, \tag{12}$$

in which $K_1 - K_4$ are functions of θ and x only. The boundary conditions are

$$\text{for } r = h_i = (R - h_2): \quad v_2 = v_i \quad \text{and} \quad w_2 = w_i, \tag{13}$$

in which u_i, v_i, and w_i are the liquid velocities at the interface between the annulus and the core layer, and

$$\text{for } r = R: \quad v_2 = 0 \quad \text{and} \quad w_2 = w_w, \tag{14}$$

where w_w is the velocity of the pipe wall. Applying Eqs. (13) and (14) to Eqs. (11) and (12) yields

$$v_2 = \frac{1}{2\eta_2}\frac{\partial\phi_2}{\partial\theta}\left\{ r\ln r - \frac{h_i^2(r^2-R^2)\ln h_i}{r(h_i^2-R^2)} - \frac{R^2(r^2-h_i^2)\ln R}{r(R^2-h_i^2)}\right\} + \frac{v_i h_i(r^2-R^2)}{r(h_i^2-R^2)} \tag{15}$$

$$w_2 = \frac{1}{4\eta_2}\frac{\partial\phi_2}{\partial x}\left\{ r^2 - R^2 + \frac{(R^2-h_i^2)\ln\dfrac{r}{R}}{\ln\dfrac{h_i}{R}}\right\} + w_i\frac{\ln\dfrac{r}{R}}{\ln\dfrac{h_i}{R}} + w_w\left(1 - \frac{\ln\dfrac{r}{R}}{\ln\dfrac{h_i}{R}}\right). \tag{16}$$

Integration of the continuity equation (1) for the annulus between its two boundaries gives the following expression:

$$\int_{h_i}^{R}\frac{\partial}{\partial r}(ru_2)dr = -h_i u_i = -\int_{h_i}^{R}\frac{\partial v_2}{\partial\theta}dr - \int_{h_i}^{R} r\frac{\partial w_2}{\partial x}dr. \tag{17}$$

Substitution of Eqs. (15) and (16) in Eq. (17) and using $h_i = R - h_2$ with $h_2 \ll R$, we find the following pressure equation for the annulus:

$$\frac{\partial}{R\,\partial\theta}\left(h_2^3\frac{\partial\phi_2}{R\,\partial\theta}\right) + \frac{\partial}{\partial x}\left(h_2^3\frac{\partial\phi_2}{\partial x}\right) = -12\eta_2 u_i - 6\eta_2 v_i\frac{\partial h_2}{R\,\partial\theta} + 6\eta_2 h_2\frac{\partial v_i}{R\,\partial\theta} + 6\eta_2(w_w - w_i)\frac{\partial h_2}{\partial x} + 6\eta_2 h_2\frac{\partial w_i}{\partial x}. \tag{18}$$

This equation can be considered as an extended version of the Reynolds equation of lubrication theory (for a detailed derivation of this equation for the case of a flow of two liquids between infinite plates, see Ooms *et al.*[19]).

B. Pressure equation for the core layer

The starting point for the pressure equation for the core layer are the equations of motion for the liquid in the core layer

$$\frac{1}{\eta_1}\frac{\partial\phi_1}{\partial r} = \frac{\partial}{\partial r}\left\{\frac{1}{r}\frac{\partial}{\partial r}(u_1 r)\right\} + \frac{1}{r^2}\frac{\partial^2 u_1}{\partial\theta^2} + \frac{\partial^2 u_1}{\partial x^2} - \frac{2}{r^2}\frac{\partial v_1}{\partial\theta}, \tag{19}$$

$$\frac{1}{\eta_1 r}\frac{\partial\phi_1}{\partial\theta} = \frac{\partial}{\partial r}\left\{\frac{1}{r}\frac{\partial}{\partial r}(v_1 r)\right\} + \frac{1}{r^2}\frac{\partial^2 v_1}{\partial\theta^2} + \frac{\partial^2 v_1}{\partial x^2} + \frac{2}{r^2}\frac{\partial u_1}{\partial\theta}, \tag{20}$$

$$\frac{1}{\eta_1}\frac{\partial\phi_1}{\partial x} = \left\{\frac{1}{r}\frac{\partial}{\partial r}\left(r\frac{\partial w_1}{\partial r}\right)\right\} + \frac{1}{r^2}\frac{\partial^2 w_1}{\partial\theta^2} + \frac{\partial^2 w_1}{\partial x^2}, \tag{21}$$

in which

$$\phi_1 = p_1 + \rho_1 g r\cos\theta, \tag{22}$$

where p_1 represents the hydrodynamic pressure in the core layer and ρ_1 is the density of the liquid in the core layer. η_1 is the dynamic viscosity of the liquid, u_1, v_1, and w_1 are the velocity components in the core layer in the radial, circumferential, and axial direction, respectively. Using the same simplification as in the preceding paragraph the equations of motion reduce to

$$\frac{\partial\phi_1}{\partial r} = 0, \tag{23}$$

$$\frac{1}{r}\frac{\partial\phi_1}{\partial\theta} = \eta_1\frac{\partial}{\partial r}\left\{\frac{1}{r}\frac{\partial}{\partial r}(v_1 r)\right\}, \tag{24}$$

$$\frac{\partial\phi_1}{\partial x} = \frac{\eta_1}{r}\frac{\partial}{\partial r}\left(r\frac{\partial w_1}{\partial r}\right). \tag{25}$$

Integration of Eqs. (24) and (25) yields

$$v_1 = \frac{1}{2\eta_1}\frac{\partial\phi_1}{\partial\theta}r\left(-\frac{1}{2} + \ln r\right) + K_5 r + \frac{K_6}{r}, \tag{26}$$

$$w_1 = \frac{1}{4\eta_1}\frac{\partial\phi_1}{\partial x}r^2 + K_7\ln r + K_8, \tag{27}$$

in which $K_5 - K_8$ are functions of θ and x only. The boundary conditions are

$$\text{for } r = h_3: \quad v_1 = 0 \quad\text{and}\quad w_1 = 0, \tag{28}$$

$$\text{for } r = h_i: \quad v_1 = v_i \quad\text{and}\quad w_1 = w_i, \tag{29}$$

in which h_3 is the distance from the interface between the solid center and the core layer to the center line of the pipe. It is important to point out, that for the case of an eccentric core h_3 is not a constant as the solid center becomes eccentric also. Applying Eqs. (28) and (29) to Eqs. (26) and (27) we find

$$v_1 = \frac{1}{2\eta_1}\frac{\partial\phi_1}{\partial\theta}\left\{ r\ln r - \frac{h_3^2(r^2-h_i^2)\ln h_3}{r(h_3^2-h_i^2)} - \frac{h_i^2(r^2-h_3^2)\ln h_i}{r(h_i^2-h_3^2)}\right\} + \frac{v_i h_i(r^2-h_3^2)}{r(h_i^2-h_3^2)}, \tag{30}$$

$$w_1 = \frac{1}{4\eta_1}\frac{\partial\phi_1}{\partial x}\left\{ r^2 - h_i^2 + \frac{(h_i^2-h_3^2)\ln\dfrac{r}{h_i}}{\ln\dfrac{h_3}{h_i}}\right\} + w_i\frac{\ln\dfrac{r}{h_3}}{\ln\dfrac{h_i}{h_3}}. \tag{31}$$

The equation of continuity reads

$$\frac{1}{r}\frac{\partial}{\partial r}(ru_1) + \frac{1}{r}\frac{\partial v_1}{\partial\theta} + \frac{\partial w_1}{\partial x} = 0, \tag{32}$$

or after integration

$$\int_0^{h_i} \frac{\partial}{\partial r}(ru_1)dr = -h_iU_i = -\int_0^{h_i} \frac{\partial v_1}{\partial \theta}dr - \int_0^{h_i} r\frac{\partial w_1}{\partial x}dr. \tag{33}$$

After substitution of Eqs. (30) and (31) in Eq. (33) and using $h_3=h_i-h_1$ with $h_1 \ll R$, we finally find the pressure equation for the core layer

$$\frac{\partial}{R\,\partial\theta}\left(h_1^3\frac{\partial\phi_1}{R\,\partial\theta}\right) + \frac{\partial}{\partial x}\left(h_1^3\frac{\partial\phi_1}{\partial x}\right) = +12\eta_1u_i - 6\eta_1v_i\frac{\partial h_1}{R\,\partial\theta} + 6\eta_1h_1\frac{\partial v_i}{R\,\partial\theta} - 6\eta_1w_i\frac{\partial h_1}{\partial x} + 6\eta_1h_1\frac{\partial w_i}{\partial x}. \tag{34}$$

C. Boundary conditions at the interface between the core layer and the annulus

At the interface between the core layer and the annulus the kinematic boundary condition holds. This condition can be written as

$$\frac{DF}{Dt} = 0, \tag{35}$$

in which

$$\frac{D}{Dt}$$

represents the material derivative and F the equation for the interface

$$F = r - h_i(\theta,x,t), \tag{36}$$

where t represents time. Substitution of Eq. (36) in Eq. (35) gives

$$u_i = \frac{v_i}{h_i}\frac{\partial h_i}{\partial\theta} + w_i\frac{\partial h_i}{\partial x} + \frac{\partial h_i}{\partial t}, \tag{37}$$

or using $h_i=R-h_2$

$$u_i = -\frac{v_i}{(R-h_2)}\frac{\partial h_2}{\partial\theta} - w_i\frac{\partial h_2}{\partial x} - \frac{\partial h_2}{\partial t}. \tag{38}$$

At the interface of the liquids also the dynamic boundary condition holds. This condition can be written as

$$(n_i\tau_{1,ik})_{r=h_i} = (n_i\tau_{2,ik})_{r=h_i}, \tag{39}$$

in which $\tau_{1,ik}$ and $\tau_{2,ik}$ represent the stress tensors for the liquid in the core layer and in the annulus, respectively. $\mathbf{n}$ is the unit vector normal to the interface. By using the basic assumptions that the thicknesses of the annulus and the core layer are small relative to the radius of the pipe and to the wavelength of a possible wave at the interface (and by applying an order of magnitude estimate for the terms as done for the derivation of the pressure equations), Eq. (39) leads to the following three conditions:

$$(p_1)_{r=h_i} = (p_2)_{r=h_i} + \sigma\left(\frac{1}{\mathbf{R_1}} + \frac{1}{\mathbf{R_2}}\right), \tag{40}$$

$$\left\{\eta_1 r\frac{\partial}{\partial r}\left(\frac{v_1}{r}\right)\right\}_{r=h_i} = \left\{\eta_2 r\frac{\partial}{\partial r}\left(\frac{v_2}{r}\right)\right\}_{r=h_i}, \tag{41}$$

$$\left(\eta_1\frac{\partial w_1}{\partial r}\right)_{r=h_i} = \left(\eta_2\frac{\partial w_2}{\partial r}\right)_{r=h_i}, \tag{42}$$

in which σ is the interfacial tension and $\mathbf{R_1}$ and $\mathbf{R_2}$ are the principal radii of curvature of the interface, to be taken as negative when the respective center of curvature falls on the side of the annular layer. Substitution of Eqs. (22) and (7) in Eq. (40) gives

$$\phi_2 = \phi_1 + \Delta\rho g h_i\cos\theta - \sigma\left(\frac{1}{\mathbf{R_1}} + \frac{1}{\mathbf{R_2}}\right), \tag{43}$$

in which $\Delta\rho=\rho_2-\rho_1$. Substitution of Eqs. (15), (16), (30), and (31) in Eqs. (41) and (42) yields (using $\eta_2/\eta_1 \ll h_2/h_1$)

$$v_i = -\frac{1}{2\eta_1}\frac{h_1^2}{h_3}\frac{\partial\phi_1}{\partial\theta} - \frac{1}{2\eta_1}\frac{h_1h_2}{R}\frac{\partial\phi_2}{\partial\theta}, \tag{44}$$

$$w_i = -\frac{1}{2\eta_1}h_1^2\frac{\partial\phi_1}{\partial x} - \frac{1}{2\eta_1}h_1h_2\frac{\partial\phi_2}{\partial x} + \frac{\eta_2}{\eta_1}\frac{h_1}{h_2}w_w. \tag{45}$$

D. Relation between pressure drop over the pipe and wall velocity

For the problem studied in this publication concerning the flow of two liquids between a solid center and a pipe wall it is of course possible to choose the pressure drop over the liquids and pipe wall velocity independent of each other. However, for a real core-annular flow with a fully liquid core surrounded by a liquid annulus a relation exists between the pressure drop and the velocity. In order to simulate a real core-annular flow as much as possible we will derive a similar relation also for the problem studied here. For that purpose we calculate first the total force F_x in the axial direction on the pipe wall (for one wavelength)

$$F_x = \int_0^{2\pi}\int_0^l \tau_{\theta x}R\,d\theta\,dx, \tag{46}$$

in which $\tau_{\theta x}$ is the shear stress at the pipe wall

$$\tau_{\theta x} = \eta_2\left(\frac{\partial w_2}{\partial r}\right)_{r=R}. \tag{47}$$

We now define the pressure drop (per wavelength) over the pipe in the following way:

$$\Delta p = F_x/(\pi R^2), \tag{48}$$

in which Δp is the difference between the pressure at $x=0$ and at $x=l$. Substitution of Eq. (16) gives

$$\Delta p = \frac{1}{\pi R^2}\int_0^{2\pi}\int_0^{l}\left\{\frac{1}{4}\frac{\partial \phi_2}{\partial x}\left(2R^2 + \frac{R_2 - h_i^2}{\ln h_i/R}\right) + \frac{\eta_2(w_i - w_w)}{\ln h_i/R}\right\}d\theta dx. \tag{49}$$

Substituting the expressions for h_i and w_i in Eq. (49) yields the relation between Δp and w_w.

E. Solution of the equations

The pressure equations for the annular layer [Eq. (18)] and for the core [Eq. (34)] together with the boundary conditions at the interface between the liquids, as formulated by Eqs. (38) and (43)–(45), form a complete description of the flow system from which in principle all possible flow patterns can be found. In our further calculations we omit the effect of the interfacial tension. So the third term on the right-hand side of Eq. (43) is neglected. We keep, of course, the buoyancy effect, as we hope to understand how this effect is counterbalanced by hydrodynamic forces. We write the relevant equations in dimensionless form. To that purpose we introduce as length scale R, as time scale $\rho_1 R^2/\eta_1$ and (hence) as the velocity scale $\eta_1/\rho_1 R$. The force scale is η_1^2/ρ_1. The following dimensionless quantities are now introduced: $H_1=h_1/R$, $H_2=h_2/R$, $H_3=h_3/R$, $H_i=h_i/R$, $X=x/R$, $T=t\eta_1/\rho_1 R^2$, $U_i=u_i\rho_1 R/\eta_1$, $V_i=v_i\rho_1 R/\eta_1$, $W_i=w_i\rho_1 R/\eta_1$, $W_w=w_w\rho_1 R/\eta_1$, $\Phi_1=\phi_1\rho_1 R^2/\eta_1^2$, and $\Phi_2=\phi_2\rho_1 R^2/\eta_1^2$. Also the following dimensionless constants are introduced: $C_1=\eta_2/\eta_1$, $C_2=\Delta\rho g R^3\rho_1/\eta_1^2$, and $C_3=\Delta p\rho_1 R^2/\eta_1^2$. The six equations can then be written as

$$\frac{\partial}{\partial\theta}\left(H_2^3\frac{\partial\Phi_2}{\partial\theta}\right) + \frac{\partial}{\partial X}\left(H_2^3\frac{\partial\Phi_2}{\partial X}\right) = -12C_1U_i - 6C_1V_i\frac{\partial H_2}{\partial\theta} + 6C_1H_2\frac{\partial V_i}{\partial\theta} - 6C_1(W_i - W_w)\frac{\partial H_2}{\partial X} + 6C_1H_2\frac{\partial W_i}{\partial X}, \tag{50}$$

$$\frac{\partial}{\partial\theta}\left(H_1^3\frac{\partial\Phi_1}{\partial\theta}\right) + \frac{\partial}{\partial X}\left(H_1^3\frac{\partial\Phi_1}{\partial X}\right) = +12U_i - 6V_i\frac{\partial H_1}{\partial\theta} + 6H_1\frac{\partial V_i}{\partial\theta} - 6W_i\frac{\partial H_1}{\partial X} + 6H_1\frac{\partial W_i}{\partial X}, \tag{51}$$

$$U_i = -\frac{V_i}{1-H_2}\frac{\partial H_2}{\partial\theta} - W_i\frac{\partial H_2}{\partial X} - \frac{\partial H_2}{\partial T}, \tag{52}$$

$$\Phi_1 = \Phi_2 - C_2H_i\cos\theta, \tag{53}$$

$$V_i = \frac{1}{(1/H_1 + C_1/H_2)}\left(-\frac{1}{2}\frac{H_1}{H_3}\frac{\partial\Phi_1}{\partial\theta} - \frac{1}{2}H_2\frac{\partial\Phi_2}{\partial\theta}\right), \tag{54}$$

$$W_i = \frac{1}{(1/H_1 + C_1/H_2)}\left(-\frac{1}{2}H_1\frac{\partial\Phi_1}{\partial X} - \frac{1}{2}H_2\frac{\partial\Phi_2}{\partial X} + \frac{C_1}{H_2}W_w\right), \tag{55}$$

in which

$$H_i = 1 - H_2 \tag{56}$$

and

$$H_1 = 1 - H_3 - H_2. \tag{57}$$

This set of equations is very similar to the one derived by Ooms *et al.*[19] for the flow of two liquids between infinite plates. It is an extended version of it. The quantities are periodic in θ with periodicity 2π. The axial pressure drop over a wavelength in the pipe is given by $\{\Phi_2(\theta,X) - \Phi_2(\theta,X+L)=C_3\}$, in which L is the ratio of the wavelength and the pipe radius. For practical applications the relevant parameters have the following values: $R\sim 10^{-1}$ m, $h_3\sim 10^{-1}$ m, $h_2\sim 10^{-2}$ m, $\rho_1\sim 10^3$ kg/m^3, $\Delta\rho\sim 10$ kg/m^3, $\eta_2\sim 10^{-3}$ kg/ms, $\eta_1\sim 10^3-1$ and $\Delta p\sim 10^{-1}$ kg/ms^2. So the constants have values of the following order of magnitude: $C_1\sim 10^{-6}-10^{-3}$, $C_2\sim 10^{-4}-10^{1}$, and $C_3\sim 10^{-5}-10^{1}$.

To eliminate U_i from the pressure equations we multiply Eq. (51) by C_1 and add it to Eq. (50). A new pressure equation is then found without U_i. Next we use Eq. (53) to eliminate Φ_1 from the new pressure equation and from Eqs. (54) and (55). The new equations for V_i and W_i (without Φ_1) are then substituted in the new pressure equation, and again another pressure equation is found. Restricting ourselves to the largest terms this last pressure equation is given by

$$\frac{\partial}{\partial\theta}\left[(H_2^3 + C_1H_1^3)\frac{\partial\Phi_2}{\partial\theta}\right] + \frac{\partial}{\partial X}\left[(H_2^3 + C_1H_1^3)\frac{\partial\Phi_2}{\partial X}\right] = 6C_1W_w\frac{\partial H_2}{\partial X} - C_1C_2H_i\left[\left\{3H_1^2 + 6\frac{H_1(H_1+H_2)}{H_3}\right\}\times\frac{\partial H_1}{\partial\theta}\sin\theta + \left\{H_1^3 + 3\frac{(H_1+H_2)H_1^2}{H_3}\right\}\cos\theta\right]. \tag{58}$$

The relation (49) between the wall velocity and the pressure drop over a wavelength of the pipe becomes in dimensionless form

$$W_w = \frac{C_3 - \dfrac{1}{2\pi}\displaystyle\int_0^{2\pi}\int_0^{L} H_2\frac{\partial\Phi_2}{\partial X}d\theta dX}{\dfrac{C_1}{\pi}\displaystyle\int_0^{2\pi}\int_0^{L}\frac{1}{H_2}d\theta dX}. \tag{59}$$

The solution procedure is now as follows:

(A) Start with a given function $H_2(\theta,X)=H_2^{(0)}-\epsilon\cos\theta + AH_2^{(1)}(X)$, in which $H_2^{(0)}$ represents the constant part of the dimensionless thickness of the annulus when there is no eccentricity, $\epsilon(<H_2^{(0)})$ is the eccentricity and $AH_2^{(1)}(X)=A\cos(2\pi X/L)$ is the periodic part of the thickness of the annulus with amplitude $A(<H_2-\epsilon)$ and dimensionless wavelength $L(=l/R)$.

(B) Calculate $H_3(\theta)=H_3^{(0)}-\epsilon\cos\theta$, in which $H_3^{(0)}$ represents the (constant) dimensionless radius of the solid center. The eccentricity is the same as for the annulus. So the distances between the solid center centerline and the interface (between the annulus and the core layer) at the top of the pipe and at the bottom are equal (see Fig. 1).

(C) Calculate $H_i = 1 - H_2$ and $H_1 = 1 - H_2 - H_3$.

(D) Choose values for C_1, C_2, and C_3.

(E) Choose an initial value for wall velocity $W_w = -(C_3/8C_1L)$ (based on a Poiseuille flow of liquid 2 through the pipe).

(F) Calculate $\partial H_2/\partial\theta$ and $\partial H_2/\partial X$ and also $\partial H_1/\partial\theta$ and $\partial H_1/\partial X$.

(G) Solve

$$\frac{\partial}{\partial\theta}\left[(H_2^3 + C_1H_1^3)\frac{\partial\Phi_2}{\partial\theta}\right] + \frac{\partial}{\partial X}\left[(H_2^3 + C_1H_1^3)\frac{\partial\Phi_2}{\partial X}\right] = f(\theta,X),$$

with

$$f(\theta,X) = 6C_1W_w\frac{\partial H_2}{\partial X} - C_1C_2H_i\left[\left\{3H_1^2 + 6\frac{H_1(H_1+H_2)}{H_3}\right\}\frac{\partial H_1}{\partial\theta}\sin\theta + \left\{H_1^3 + 3\frac{(H_1+H_2)H_1^2}{H_3}\right\}\cos\theta\right].$$

Φ_2 is a periodic function of θ with periodicity 2π. Φ_2 is also a periodic function of X with periodicity L and $\{\Phi_2(\theta,X) - \Phi_2(\theta,X+L) = C_3\}$.

(H) Calculate $\Phi_1(\theta,X) = \Phi_2(\theta,X) - C_2H_i\cos\theta$.

(I) Calculate $\partial\Phi_2/\partial\theta$ and $\partial\Phi_2/\partial X$ and also $\partial\Phi_1/\partial\theta$ and $\partial\Phi_1/\partial X$.

(J) Calculate

$$V_i = \frac{1}{(1/H_1 + C_1/H_2)}\left(-\frac{1}{2}\frac{H_1}{H_3}\frac{\partial\Phi_1}{\partial\theta} - \frac{1}{2}H_2\frac{\partial\Phi_2}{\partial\theta}\right)$$

and

$$W_i = \frac{1}{(1/H_1 + C_1/H_2)}\left(-\frac{1}{2}H_1\frac{\partial\Phi_1}{\partial X} - \frac{1}{2}H_2\frac{\partial\Phi_2}{\partial X} + \frac{C_1}{H_2}W_w\right).$$

(K) Calculate

$$U_i = \frac{1}{12}\left\{\frac{\partial}{\partial\theta}\left(H_1^3\frac{\partial\Phi_1}{\partial\theta}\right) + \frac{\partial}{\partial X}\left(H_1^3\frac{\partial\Phi_1}{\partial X}\right)\right\} + \frac{1}{12}\left\{+6V_i\frac{\partial H_1}{\partial\theta} - 6H_1\frac{\partial V_i}{\partial\theta} + 6W_i\frac{\partial H_1}{\partial X} - 6H_1\frac{\partial W_i}{\partial X}\right\}.$$

(L) Calculate

$$\frac{\partial H_2}{\partial T} = -U_i - \frac{V_i}{1-H_2}\frac{\partial H_2}{\partial\theta} - W_i\frac{\partial H_2}{\partial X}.$$

(M) Calculate the new annular thickness

$$H_2 = H_2^{\text{old}} + \frac{\partial H_2}{\partial T}\Delta T,$$

in which ΔT is a time step.

(N) Calculate the new wall velocity based on Eq. (59),

$$W_w = \frac{C_3 - \frac{1}{2\pi}\int_0^{2\pi}\int_0^L H_2\frac{\partial\Phi_2}{\partial X}d\theta dX}{\frac{C_1}{\pi}\int_0^{2\pi}\int_0^L \frac{1}{H_2}d\theta dX}.$$

(O) Calculate the vertical force F_{up} on the core (solid center and liquid core layer) due to buoyancy and hydrodynamic forces. The derivation of F_{up} is given in the Appendix and the result is

$$F_{\text{up}} = -\int_0^{2\pi}d\theta\int_0^L dX[\Phi_2\cos\theta] - \int_0^{2\pi}d\theta\int_0^L dX\left[\left\{+\frac{1}{2}\frac{\partial\Phi_2}{\partial\theta}H_2 - C_1\frac{V_i}{H_2}\right\}\sin\theta\right] + \frac{1}{2}C_2\int_0^{2\pi}d\theta\int_0^L dX[(1-H_2)^2]. \tag{60}$$

(P) Calculate the new eccentricity ϵ because of the vertical movement of the core due to the vertical force.

(Q) Calculate the new position of the surface of the solid center $H_3 = H_3^{(0)} - \epsilon\cos\theta$. Assuming that the distances between the solid center centerline and the interface (between the annulus and the core layer) at the top of the pipe and at the bottom are equal, calculate also the new values for H_2, H_1, and H_i.

(R) Go back to (F).

III. NUMERICAL SOLUTION METHOD

In order to obtain the solution of the problem posed in Sec. II, it appears that the most challenging part is to find the solution of Eq. (58) together with the boundary conditions. For a general function H_2 it is impossible to find an analytic expression for the pressure Φ_2.

For the solution of the flow problem we use the solution procedure given in the preceding section. For the discretization we use n_t grid points in the θ-direction and n_x grid points in the X-direction. This leads to the following step sizes: $h_t = 2\pi/n_t$ and $h_x = L/n_x$. The grid points are located at $\theta_i = (i-1)h_t$ and $X_j = (j-1)h_x$. Furthermore, $\Phi_2(t,X)$ is approximated by the grid function Φ_{2h}, such that

$$\Phi_2(t_i,X_j) \approx \Phi_{2h}(i,j).$$

All functions are periodic in θ and X, except Φ_1 and Φ_2, which are periodic in θ, but periodic up to a constant in X:

$$\Phi_2(0,X) = \Phi_2(2\pi,X), \quad X \in [0,L]$$

and

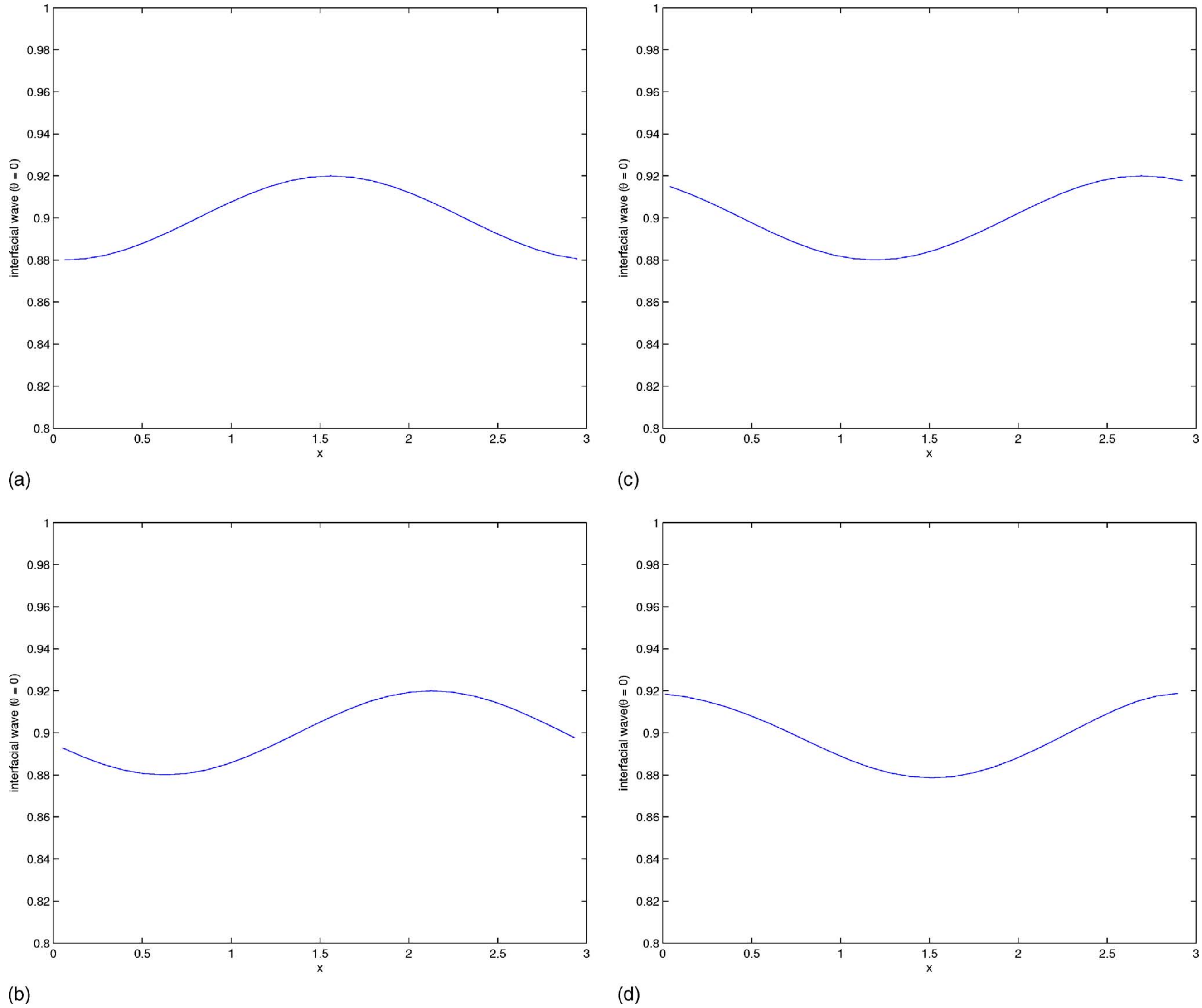

FIG. 2. (Color online) Movement of wave at the interface (at the top of the pipe) as a function of time. Concentric core at $T=0$. No density difference between core and annulus. Pressure gradient over pipe. (a) After 0 time steps; (b) after 30 time steps; (c) after 60 time steps; and (d) after 90 time steps. $C_1=10^{-4}$, $C_2=0$, $C_3=10^{-2}$, $\Delta T=10^{-2}$, $H_2^{(0)}=0.1$, $H_3^{(0)}=0.8$, $A=0.02$, $\epsilon=0$, $L=3$, $n_x=26$ and $n_t=20$. The pipe wall is at rest according to the chosen reference system.

$$\Phi_2(\theta,0) = \Phi_2(\theta,L) + C_3, \quad \theta \in [0,2\pi].$$

Numerically, this is implemented as

$$\Phi_{2h}(1,j) = \Phi_{2h}(n_t+1,j), \quad \text{for } j \in [0,n_x+1], \tag{61}$$

$$\Phi_{2h}(i,1) = \Phi_{2h}(i,n_x+1) + C_3, \quad \text{for } i \in [0,n_t+1]. \tag{62}$$

In order to approximate the first and second order derivatives, we use central differences. For points on the boundaries the central differences are combined with the periodical boundary conditions.

As already said the most important part of the calculation procedure is the solution of Eq. (58) together with the boundary conditions. It is easy to see that a pressure function Φ_2 satisfying this problem is determined up to a constant. So, if $\Phi_2(\theta,X)$ is a solution, then $\Phi_2(\theta,X)+C$ is also a solution for an arbitrary constant $C \in \mathbb{R}$. This means that the continuous problem does not have a unique solution. Furthermore, the solution only exists if the right-hand-side function f_6 satisfies a compatibility equation. After integration of Eq. (58) with respect to θ and X it can easily be proved that the left-hand side is equal to zero. So this must also hold for the right-hand side and therefore as compatibility condition the following expression is chosen:

$$\int_0^{2\pi} d\theta \int_0^L dX[f(\theta,X)] = 0. \tag{63}$$

The same problem exists for the discretized equations. After discretization of Eq. (58) one has to solve the linear system

$$A\mathbf{x} = \mathbf{b}, \tag{64}$$

where $\mathbf{x} \in \mathbb{R}^N$, with $N=(n_t+1)\cdot(n_x+1)$. Grid function Φ_{2h} and $\mathbf{x}$ are related by

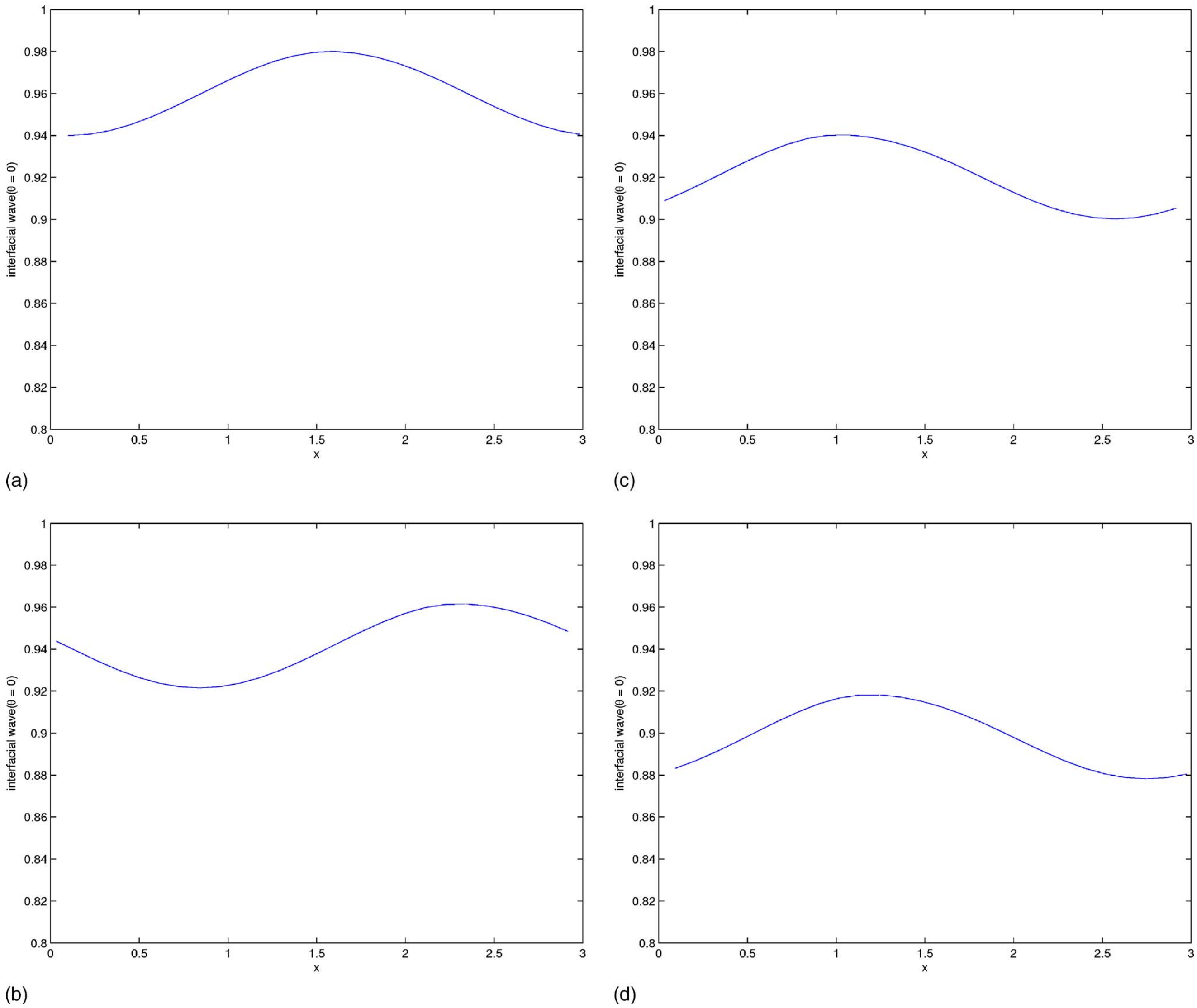

FIG. 3. (Color online) Movement of wave at the interface at the top of the pipe as a function of time. Eccentric core at $T=0$. No density difference between core and annulus. Pressure gradient over pipe. (a) After 0 time steps; (b) after 45 time steps; (c) after 135 time steps; and (d) after 1500 time steps. $C_1=10^{-4}$, $C_2=0$, $C_3=10^{-2}$, $\Delta T=10^{-2}$, $H_2^{(0)}=0.1$, $H_3^{(0)}=0.8$, $A=0.02$, $\epsilon=0.06$, $L=3$, $n_x=26$, and $n_t=20$. The pipe wall is at rest according to the chosen reference system.

$$\Phi_{2h}(i,j)=\mathbf{x}(i+(j-1)n_t).$$

It appears that $\det(A)=0$, so the matrix is singular. If function f satisfies the compatibility condition, the linear system should also have a solution, which is determined up to a constant. Due to discretization and rounding errors it is possible that $\mathbf{b}$ does not satisfy the following discrete compatibility condition exactly:

$$\mathbf{b}^T\mathbf{y}=\mathbf{0} \quad \text{for } \mathbf{y} \quad \text{such that} \quad A^T\mathbf{y}=\mathbf{0}, \tag{65}$$

(see p. 139 of Strang[20] and Sec. 8.3.4 of Elman *et al.*[21]). For this reason we solve Eq. (64) as follows:

- Determine the left eigenvector $\mathbf{y}$ of A corresponding to the zero eigenvalue, so

$$A^T\mathbf{y}=\mathbf{0}.$$

- Adapt $\mathbf{b}$:

$$\mathbf{b}=\mathbf{b}-\frac{\mathbf{b}^T\mathbf{y}}{\mathbf{y}^T\mathbf{y}}\mathbf{y},$$

such that it satisfies the compatibility equation (65).
- Solve the resulting linear system by the GMRES method (for more details, see Refs. 22 and 23).

We use GMRES instead of Gaussian elimination for the following reasons:

- GMRES is a more efficient method than Gaussian elimination for large sparse matrices.
- The GMRES method can be applied to a singular system (see Ref. 24), whereas Gaussian elimination can only be used for a nonsingular system.

Another idea is to regularize matrix A. A possibility is to replace A by $(A-uu^T)$, where u is the unit eigenvector cor-

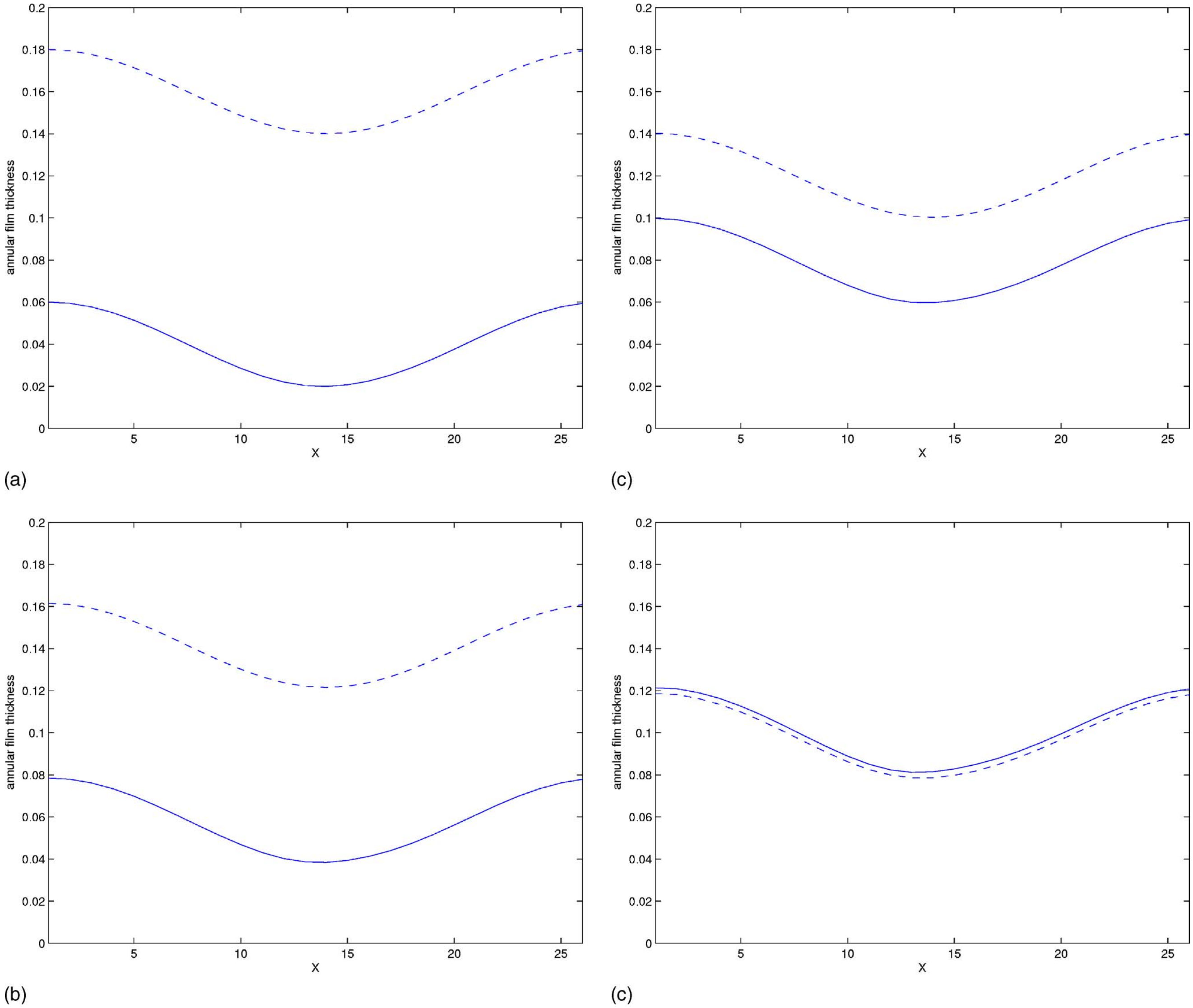

FIG. 4. (Color online) Thickness of annular layer at the top of the pipe (full line) and at the bottom (dotted line) as a function of time. Eccentric core at $T=0$. No density difference between core and annulus. Pressure gradient over pipe. (a) After 0 time steps; (b) after 45 time steps; (c) after 135 time steps; and (d) after 1500 time steps. $C_1=10^{-4}$, $C_2=0$, $C_3=10^{-2}$, $\Delta T=10^{-2}$, $H_2^{(0)}=0.1$, $H_3^{(0)}=0.8$, $A=0.02$, $\epsilon=0.06$, $L=3$, $n_x=26$, and $n_t=20$. The solid center is at rest according to the chosen reference system.

responding to the zero eigenvalue. It is easy to see that the zero eigenvalue of A is replaced by an eigenvalue equal to 1. Now Gaussian elimination can be applied to $(A-uu^T)$. A drawback of this approach is that $(A-uu^T)$ is a full matrix, whereas A is a sparse matrix. This leads to very high memory and CPU time costs for this approach.

The other parts of the solution procedure are straightforward to discretize. For the postprocessing we have to compute the upward vertical force on the core. This is done by applying the trapezoidal integration method to Eq. (60).

IV. RESULTS

A. No density difference between core and annulus

We begin by investigating the development of the wave at the interface between the core layer and the annulus for the case that the densities of the liquids in the core layer and annulus are the same ($C_2=0$). The ratio of the viscosity of the liquid in the annulus and in the core is assumed to be 10^{-4} (so $C_1=10^{-4}$). The pressure drop in the X-direction is chosen to be $C_3=10^{-2}$. For the thickness of the annular layer we choose $H_2^{(0)}=0.1$, for the thickness of the solid center $H_3^{(0)}=0.8$, for the amplitude $A=0.02$, and for the wavelength $L=3$. We start with a concentric position of the core ($\epsilon=0$). In Fig. 2 we show the position and the shape of the wave at four different values of dimensionless time T. A reference system is chosen as the one, according to which the pipe wall is at rest (and so according to which the solid center moves). As expected the wave propagates in the downstream direction with the flow of the core layer. We found that the wave shape does not change in this case. At the small viscosity ratio of 10^{-4} the interfacial wave tends to a standing wave convected with the velocity of the flow at the interface between the core layer and the annular layer and the growth rate is zero. This is in agreement with the results of Hu *et al.*[25]

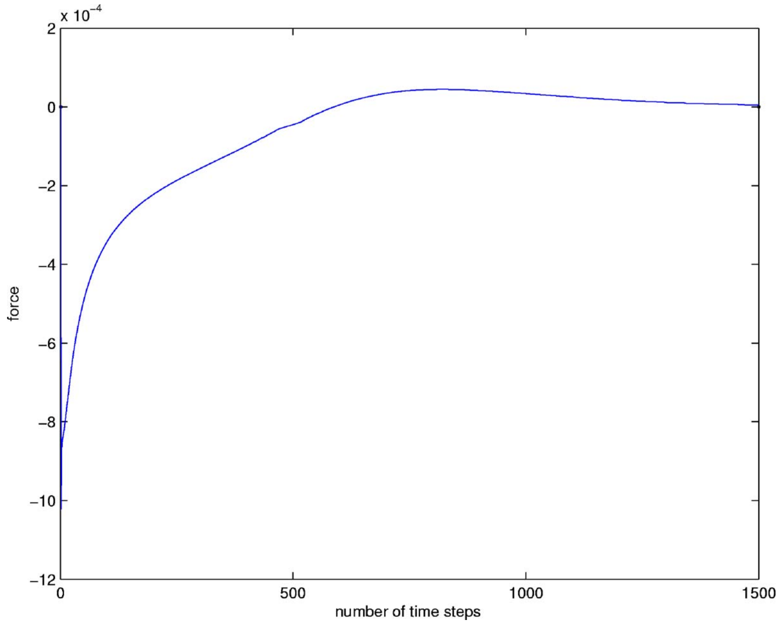

FIG. 5. (Color online) Vertical force on core as a function of time.

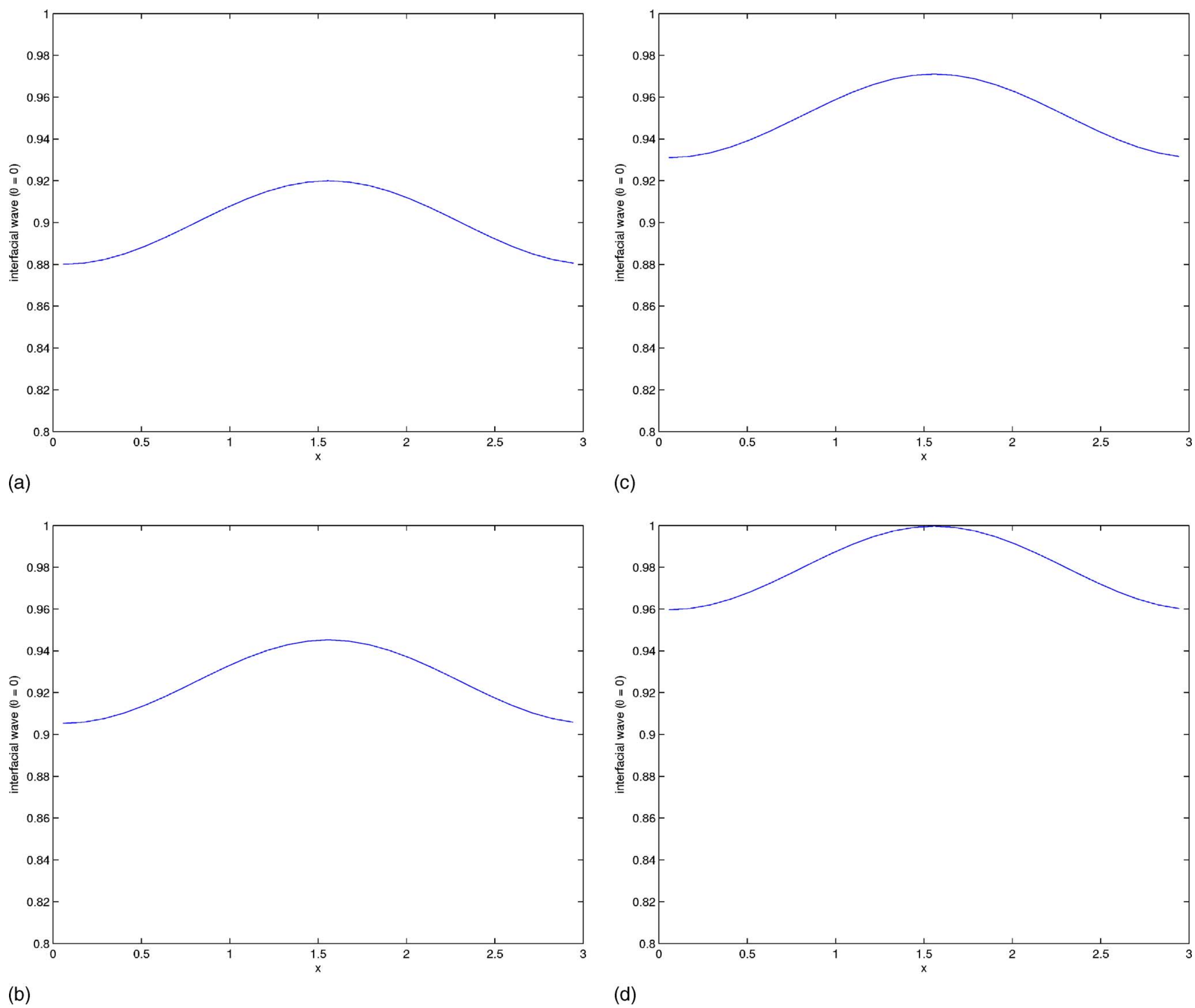

FIG. 6. (Color online) Position of wave at the interface (at top of the pipe) as a function of time. Concentric core at $T=0$. Density difference between core and annulus. No pressure gradient over pipe. (a) After 0 time steps; (b) after 9 time steps; (c) after 18 time steps; and (d) after 27 time steps. $C_1=10^{-4}$, $C_2=10^{-3}$, $C_3=0$, $\Delta T=10^{-3}$, $H_2^{(0)}=0.1$, $H_3^{(0)}=0.8$, $A=0.02$, $\epsilon=0$, $L=3$, $n_x=26$, and $n_t=20$. The pipe wall and solid center are at rest according to the chosen reference system.

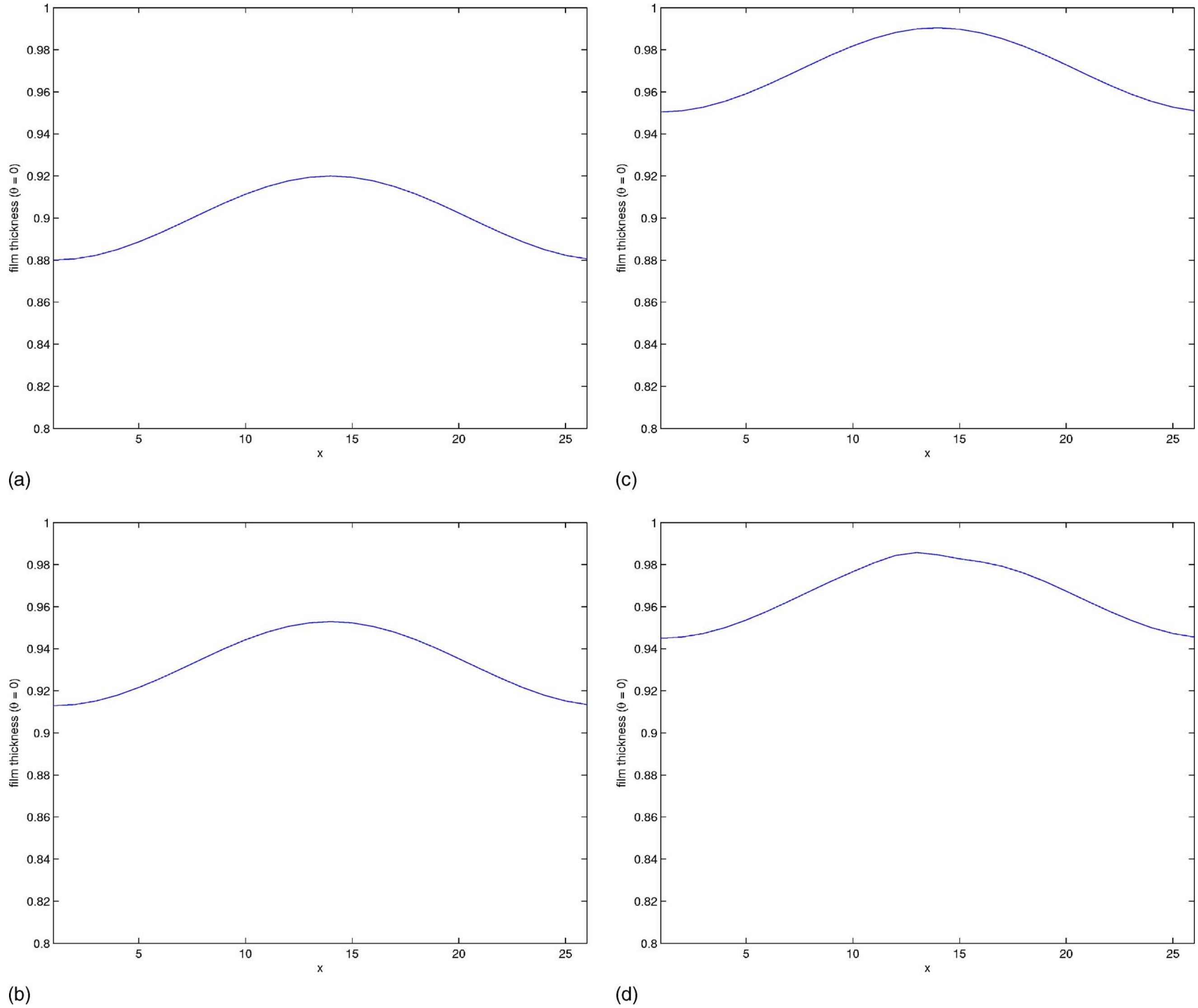

FIG. 7. (Color online) Movement of wave at the interface (at top of the pipe) as a function of time. Concentric core at $T=0$. Density difference between core and annulus. Pressure gradient over pipe. (a) After 0 time steps; (b) after 70 time steps; (c) after 150 time steps; and (d) after 500 time steps. $C_1=10^{-4}$, $C_2=10^{-3}$, $C_3=10^{-2}$, $\Delta T=10^{-3}$, $H_2^{(0)}=0.1$, $H_3^{(0)}=0.8$, $A=0.02$, $\epsilon=0$, $L=3$, $n_x=26$, and $n_t=20$. The solid center is at rest according to the chosen reference system.

Next we change the initial eccentricity of the core, keeping all other parameters the same as for the concentric case. For the initial eccentricity the following value was chosen: $\epsilon=0.06$. After the start of the calculation the hydrodynamic force on the core pushed it back into a concentric position. In Fig. 3 the position of the interfacial wave is given for four values of time. A reference system is chosen as the one, according to which the pipe wall is at rest. It is clear that the interface is moving away from the wall toward a concentric position. The interfacial wave moves forward and changes only slightly. In Fig. 4 we show the thickness of the annular layer at the top of the pipe ($\theta=0$) and at the bottom ($\theta=\pi$). For this figure the reference system is the one according to which the solid center is at rest. As can be seen the thickness at the top and at the bottom become equal after some time. They are also not shifted with respect to each other in the axial direction. So the interfacial wave remains cylindrically symmetric. In Fig. 5 the vertical force on the core is shown as a function of time. It quickly becomes negative, thus pushing the core downward. When the core gets into a concentric position (there is no buoyancy) the force disappears. In the next paragraph we will discuss in more detail the reason for the vertical force.

B. Density difference between core and annulus

In the following step we investigate the interesting case of core-annular flow with a density difference between the core and the annular layer. We start our calculation for the case, that there is no pressure gradient over the pipe ($C_3=0$). For the buoyancy parameter we choose a value of $C_2=10^{-3}$. All other parameters are the same as for the case of a concentric core without density difference and with pressure gradient. The result is shown in Fig. 6. In this figure the position of the wave at the top of the pipe is given as a function of time. The curved line represents again the wave at the interface between the core layer and the annular layer; the horizontal top line represents the pipe surface. So the

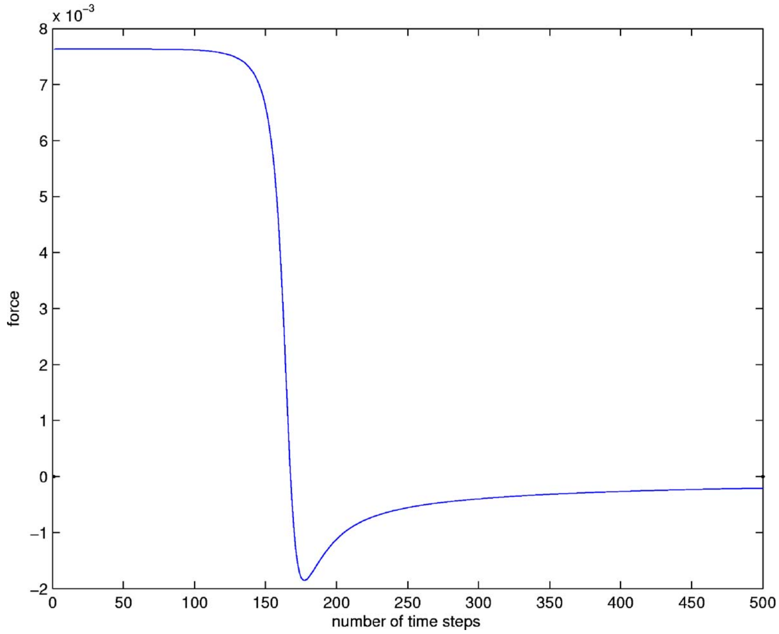

FIG. 8. (Color online) Vertical force on core as a function of time.

distance between these two lines represents the annular thickness. As expected the core rises in the pipe due to the buoyancy force and touches the top of the pipe.

Next we treat the complete problem: core-annular flow with a density difference between the core and the annular layer and with a pressure gradient over the pipe. To that purpose the (dimensionless) pressure gradient is increased from $C_3=0$ to $C_3=10^{-2}$ and all other parameters are kept the same. In practice it is found that for this case an eccentric core-annular flow (rather than a stratified flow) develops in time, and it is interesting to see whether this observation also results from our calculation. The results are given in Fig. 7. Again in this figure the curved line represents the interface between the core layer and the annular layer; the horizontal top line is the pipe surface. So the distance between these two lines represents the annular thickness. As can be seen this thickness remains finite as a function of time; the core does not touch the upper pipe wall. A balance develops between the buoyancy force and the hydrodynamic force, that makes a steady eccentric core-annular flow possible. This can also be seen from Fig. 8, which gives the vertical force on the core as a function of time for the case of Fig. 7. At first it is positive because of the buoyancy. However, the hydrodynamic force develops due to a change in the wave profile (see Fig. 7) and the total vertical force on the core decreases. After a certain time it becomes zero, which means that a steady core-annular flow is achieved.

As mentioned the development of the hydrodynamic force is due to a change in the wave profile, in particular at the top of the pipe where the annular thickness is small. As can be seen from Fig. 7 the wave develops in such a manner, that it is no longer symmetric in the axial direction. On the right-hand side of the wave top the wave shape becomes wedge-shaped. This is not the case on the left-hand side of the wave top. Due to the wave velocity in the (positive) axial direction a strong pressure built-up takes place at the wedge-shaped part of the wave, which is larger than the pressure on the left-hand side. So a net downward vertical force on the core is generated, which balances the buoyancy force when steady state has been reached. The important point is, that this wedged-shaped wave part develops automatically.

We have repeated this calculation many times for different values of the parameters and always found the same type of result. Another example is given in Fig. 9 with Fig. 10 for the vertical force. In this case the viscosity ratio is lower, $C_1=10^{-3}$; the density difference is larger $C_2=2\cdot 10^{-3}$; and the pressure gradient is larger $C_3=7\cdot 10^{0}$. The development of the nonsymmetrical wave shape in the axial direction can again be observed. After some time it has developed so much, that the buoyancy force is counterbalanced and a steady core-annular flow is present. The final average thickness of the annular layer at the top of the pipe depends on the value of the relevant parameters. For instance, the core eccentricity decreases with increasing pressure gradient and with decreasing density difference.

We have compared predictions made with the model with an oil-water core-annular flow experiment described by Oliemans and Ooms[2] in their review paper. The experiment was performed in a 9 m long horizontal perspex pipe of 2 in. diam. The difference in density between water and oil was about 30 kg/m^3. The amount of water was 20%. The oil viscosity was 3300 cP, and the oil velocity was 1 m/s. Oil and water were introduced into the pipe via an inlet device that consisted of a central tube surrounded by an annular slit. The oil was supplied via the tube, and the water via the slit. Immediately after the inlet device a wave appeared at the oil-water interface. Its wavelength was of the same order of magnitude as the radius of the pipe. For this set of conditions stable core-annular flow was found to be possible. However, the position of the oil core was very eccentric. So the thickness of the annular layer at the top of the pipe was much smaller than the annular thickness at the bottom. (Most of the water was at the lower part of the pipe.) We have simulated this experiment with our model by using the values of the

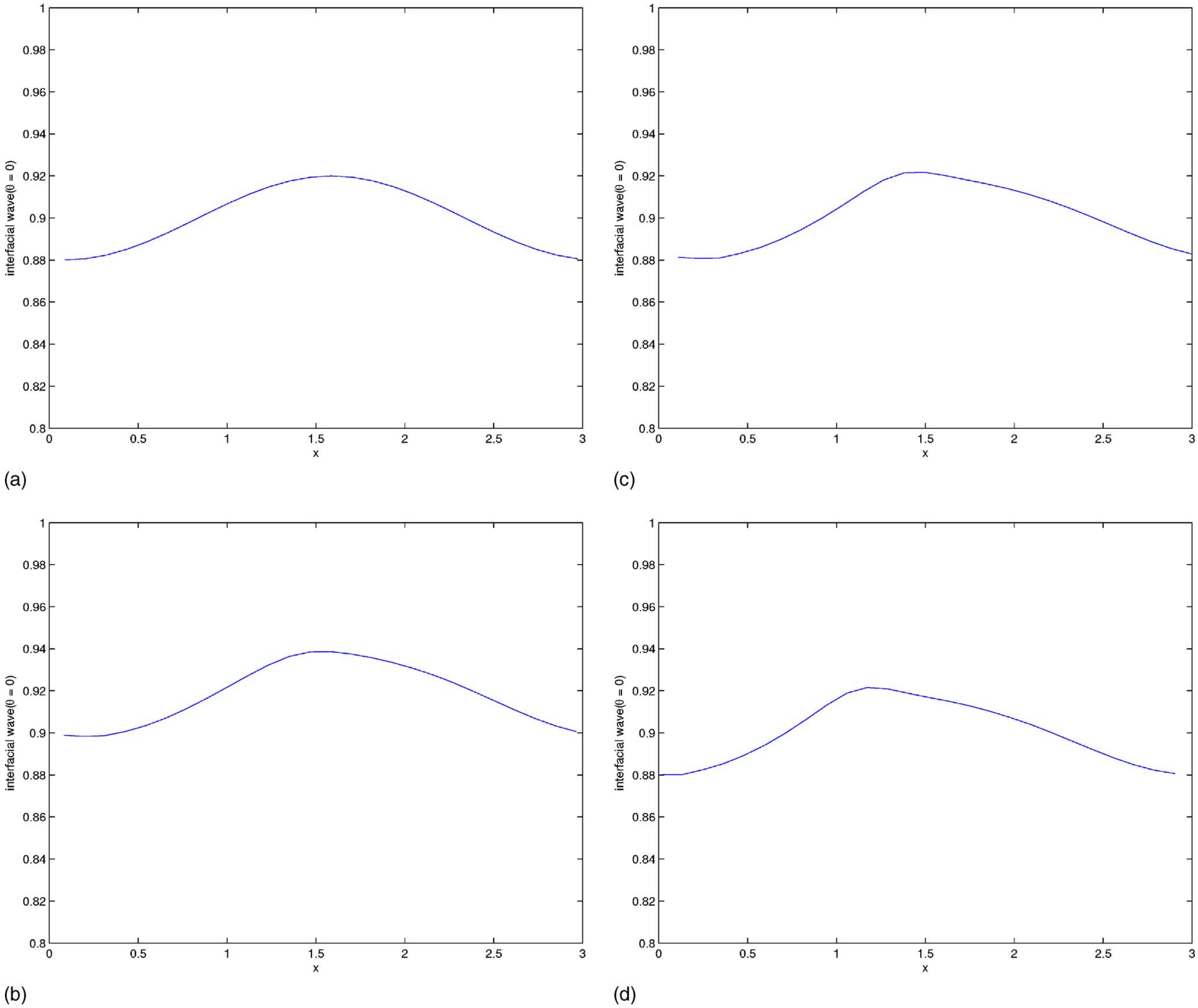

FIG. 9. (Color online) Movement of the wave at the interface (at top of the pipe) as a function of time. Concentric core at $T=0$. Density difference between core and annulus. Pressure gradient over pipe. (a) After 0 time steps; (b) after 240 time steps; (c) after 690 time steps; and (d) after 900 time steps. $C_1=10^{-3}$, $C_2=2.10^{-3}$, $C_3=7.10^{0}$, $\Delta T=10^{-4}$, $H_2^{(0)}=0.1$, $H_3^{(0)}=0.8$, $A=0.02$, $\epsilon=0$, $L=3$, $n_x=26$, and $n_t=20$. The solid center is at rest according to the chosen reference system.

relevant parameters given above. We paid special attention to the levitation capacity of core-annular flow. To that purpose we started the calculation with a flow without density difference between water and oil ($\Delta\rho=0$ kg/m^3). Thereafter we gradually increased the value of $\Delta\rho$ and studied its influence on the distance Δd between the top of the wave (at the interface between the water layer and the oil layer) and the pipe wall at the top of the pipe. The result of the calculation is given in Fig. 11. Without a density difference $\Delta d=1.5$ mm. However with increasing value of $\Delta\rho$ the value of Δd decreases rather quickly. At $\Delta\rho=30$ kg/m^3 we calculated $\Delta d=0.42$ mm. So according to our model core-annular flow still exists at $\Delta\rho=30$ kg/m^3, although the annular water layer has become very thin at the top of the pipe. Considering the approximations made in our theoretical model we feel encouraged by this result.

V. CONCLUSION

Our calculation has confirmed the experimental observation, that core-annular flow (with a density difference between the high-viscosity core and the low-viscosity annulus) through a horizontal pipe is possible. When the pressure gradient over the pipe is large enough, a balance develops between the buoyancy force and the hydrodynamic force on the core that makes eccentric core-annular flow possible. With decreasing pressure gradient or increasing buoyancy force the eccentricity of the core increases.

In this publication the core is assumed to consist of a solid center surrounded by a high-viscosity liquid layer. The reason is, as mentioned before, that we cannot solve the problem in which the complete core has a finite viscosity by means of the partly analytical and partly numerical method that we applied in this publication. To the best of our knowl-

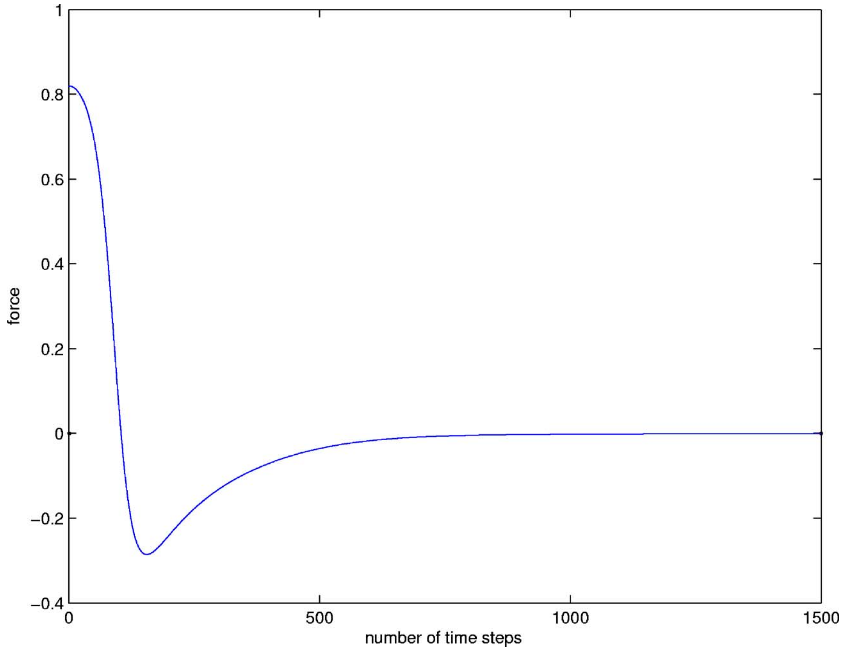

FIG. 10. (Color online) Vertical force on the core as a function of time.

edge the problem of a (lubricating) low-viscosity liquid layer on the outside of a high-viscosity core (single core fluid without solid center) with a density difference between the two liquids moving through a horizontal pipe has also not been solved numerically. In a recent publication by Kang, Shim, and Osher[26] level set based simulations of a two-phase oil-water flow through a pipe is made. For the case of an upward or downward core-annular flow through a vertical pipe they incorporate the buoyancy force due to a density difference between water and oil in their simulations. However, for the case of a horizontal pipe the buoyancy force is neglected, as Kang, Shim, and Osher solve an axisymmetric flow problem.

ACKNOWLEDGMENTS

The authors are grateful for stimulating discussions with Dr. Ir. B. J. Boersma and Dr. Ir. M. J. B. M. Pourquie of the Laboratory for Aero- and Hydrodynamics of the Delft University of Technology.

APPENDIX: DERIVATION OF THE VERTICAL FORCE ON THE CORE

The total force on the core (solid center and core layer) in the i-direction is given by

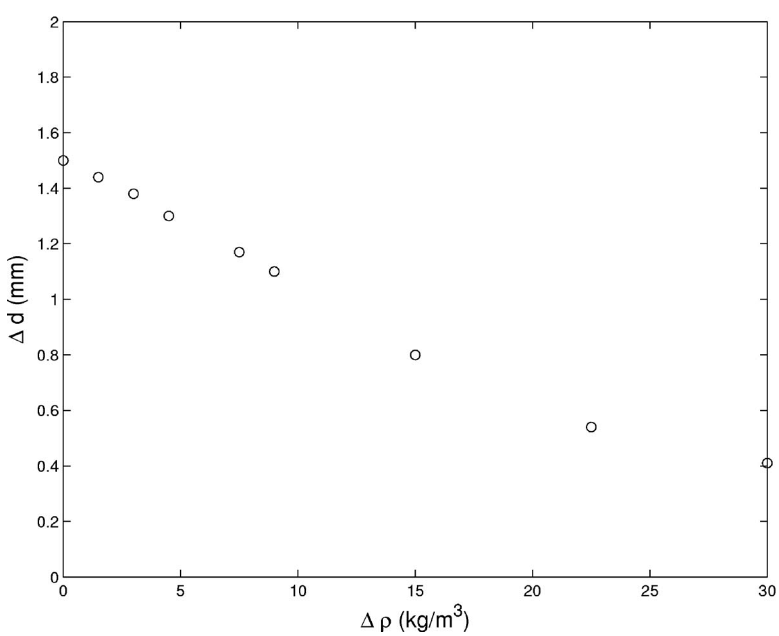

FIG. 11. Distance between the wave top at the oil-water interface and pipe wall.

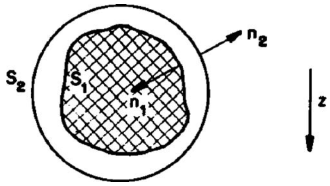

FIG. 12. Cross section of the core-annular flow.

$$F_i^{\text{core}} = \int_{S_1} (p_2\delta_{ik} - \tau_{2,ik}^{(v)})_{S_1} n_{1,k} dS_1 + \int_{S_5} p_1 \delta_{ix} dS_5 - \int_{S_6} p_1 \delta_{ix} dS_6 + \rho_1 g Q_1 \delta_{i,z}, \tag{A1}$$

in which x is the axial direction, z is the downward vertical direction, S_1 is the side surface of the core as shown in Fig. 12, S_5 and S_6 are the cross-sectional surface areas of the core at x and $x+l$, $n_{1,k}$ is the normal on the core as shown in the figure, $\tau_{2,ik}^{(v)}$ is the viscous part of the stress tensor, and Q_1 is the core volume inside the surfaces S_1, S_5, and S_6. As the integral at S_1 are difficult to evaluate, we will express the force on the core in terms of integrals at the pipe surface S_2. To that purpose we first calculate the total force exerted on the annular layer, which is equal to

$$F_i^{\text{ann}} = - \int_{S_1} (p_2\delta_{ik} - \tau_{2,ik}^{(v)})_{S_1} n_{1,k} dS_1 - \int_{S_2} (p_2\delta_{ik} - \tau_{2,ik}^{(v)})_{S_2} n_{2,k} dS_2 + \int_{S_3} p_2 \delta_{ix} dS_3 - \int_{S_4} p_2 \delta_{ix} dS_4 + \rho_2 g Q_2 \delta_{iz}, \tag{A2}$$

where $n_{2,k}$ is the normal on the pipe wall as shown in the figure, S_3 and S_4 are the cross-sectional surface areas of the annulus at x and $x+l$ and Q_2 is the annular volume inside the surfaces S_1, S_2, S_3, and S_4. At equilibrium the forces on the annulus balance each other, so $F_i^{\text{ann}}=0$. This yields the following relation:

$$\int_{S_1} (p_2\delta_{ik} - \tau_{2,ik}^{(v)})_{S_1} n_{1,k} dS_1 = - \int_{S_2} (p_2\delta_{ik} - \tau_{2,ik}^{(v)})_{S_2} n_{2,k} dS_2 + \int_{S_3} p_2 \delta_{ix} dS_3 - \int_{S_4} p_2 \delta_{ix} dS_4 + \rho_2 g Q_2 \delta_{iz}. \tag{A3}$$

Substitution of Eq. (A3) in Eq. (A1) gives

$$F_i^{\text{core}} = - \int_{S_2} (p_2\delta_{ik} - \tau_{2,ik}^{(v)})_{S_2} n_{2,k} dS_2 + \rho_2 g (Q_1 + Q_2)\delta_{iz} - \Delta\rho g Q_1 \delta_{i,z} + \int_{S_3} p_2 \delta_{ix} dS_3 - \int_{S_4} p_2 \delta_{ix} dS_4 + \int_{S_5} p_1 \delta_{ix} dS_5 - \int_{S_6} p_1 \delta_{ix} dS_6. \tag{A4}$$

Consequently, for $i=z$ Eq. (A4) reduces to

$$F_z^{\text{core}} = R\int_0^{2\pi} d\theta \int_0^l dx (p_2)_{r=R} \cos\theta + \eta_2 R \int_0^{2\pi} d\theta \int_0^l dx \left\{ r\frac{\partial}{\partial r}\left(\frac{v_2}{r}\right)\right\}_{r=R} \sin\theta + \rho_2 g R^2 \int_0^{2\pi} d\theta \int_0^l dx \cos^2\theta - \frac{\Delta\rho g}{2}\int_0^{2\pi} d\theta \int_0^l dx h_1^2, \tag{A5}$$

or using Eq. (7),

$$F_z^{\text{core}} = R\int_0^{2\pi} d\theta \int_0^l dx (\phi_2)_{r=R} \cos\theta + \eta_2 R \int_0^{2\pi} d\theta \int_0^l dx \left\{ r\frac{\partial}{\partial r}\left(\frac{v_2}{r}\right)\right\}_{r=R} \sin\theta - \frac{\Delta\rho\, g}{2}\int_0^{2\pi} d\theta \int_0^l dx h_1^2. \tag{A6}$$

Substitution of Eq. (15) in Eq. (A6), keeping only the largest terms and making the result dimensionless yields after some calculations the following expression for the upward vertical force on the core:

$$F_{\text{up}} = F_{-z}^{\text{core}} = - \int_0^{2\pi} d\theta \int_0^L dX [\Phi_2 \cos\theta] - \int_0^{2\pi} d\theta \int_0^L dX \left[\left\{ + \frac{1}{2}\frac{\partial \Phi_2}{\partial\theta} H_2 - C_1 \frac{V_i}{H_2}\right\}\sin\theta\right] \times \frac{1}{2} C_2 \int_0^{2\pi} d\theta \int_0^L dX[(1-H_2)^2]. \tag{A7}$$

[1]D. D. Joseph and Y. Y. Renardy, *Fundamentals of Two-Fluid Dynamics, Part II: Lubricated Transport, Drops and Miscible Liquids* (Springer-Verlag, New York, 1993).

[2]R. V. A. Oliemans and G. Ooms, "Core-annular flow of oil and water through a pipeline," in *Multiphase Science and Technology*, edited by G. F. Hewitt, J. M. Delhaye, and N. Zuber (Hemisphere, Washington, D.C., 1986), Vol. 2.

[3]D. D. Joseph, R. Bai, K. P. Chen, and Y. Y. Renardy, "Core-annular flows," Annu. Rev. Fluid Mech. **29**, 65 (1999).

[4]G. Ooms, "The hydrodynamic stability of core-annular flow of two ideal liquids," Appl. Sci. Res. **26**, 147 (1972).

[5]R. Bai, K. Chen, and D. D. Joseph, "Lubricated pipelining: Stability of

core-annular flow. Part 5. Experiments and comparison with theory," J. Fluid Mech. **240**, 97 (1992).
[6] R. Bai, K. Kelkar, and D. D. Joseph, "Direct simulation of interfacial waves in a high-viscosity-ratio and axisymmetric core-annular flow," J. Fluid Mech. **327**, 1 (1996).
[7] Y. Y. Renardy, "Snakes and corkscrews in core-annular down-flow of two liquids," J. Fluid Mech. **340**, 297 (1997).
[8] J. Li and Y. Y. Renardy, "Direct simulation of unsteady axisymmetric core-annular flow with high viscosity ratio," J. Fluid Mech. **391**, 123 (1999).
[9] C. Kouris and J. Tsamopoulos, "Dynamics of axisymmetric core-annular flow in a straight tube. I. The more viscous fluid in the core, bamboo waves," Phys. Fluids **13**, 841 (2001).
[10] T. Ko, H. G. Choi, R. Bai, and D. D. Joseph, "Finite element method simulation of turbulent wavy core-annular flows using a $k-\omega$ turbulence model method," Int. J. Multiphase Flow **28**, 1205 (2002).
[11] G. Ooms, "Fluid-mechanical studies on core-annular flow," Ph.D. thesis, Delft University of Technology (1971).
[12] G. Ooms and H. L. Beckers, "The flow of a rigid core surrounded by an annular liquid layer through a horizontal tube," Appl. Sci. Res. **26**, 321 (1972).
[13] G. Ooms, A. Segal, A. J. van der Wees, R. Meerhoff, and R. V. A. Oliemans, "A theoretical model for core-annular flow of a very viscous oil core and a water annulus through a horizontal pipe," Int. J. Multiphase Flow **10**, 41 (1984).
[14] R. V. A. Oliemans, "The lubricating-film model for core-annular flow," Ph.D. thesis, Delft University of Technology (1986).
[15] G. Ooms and P. Poesio, "Stationary core-annular flow through a horizontal pipe," Phys. Rev. E **68**, 066301 (2003).
[16] A. C. Bannwarth, "Bubble analogy and stabilization of core-annular flow," J. Energy Resour. Technol. **123**, 127 (2001).
[17] D. T. Papageorgiou, C. Maldarelli, and D. S. Rumschitzki, "Nonlinear interfacial stability of core-annular film flows," Phys. Fluids A **2**, 340 (1990).
[18] H. H. Wei and D. S. Rumschitzki, "The linear stability of a core-annular flow in an asymptotically corrugated tube," J. Fluid Mech. **466**, 113 (2002).
[19] G. Ooms, A. Segal, S. Y. Cheung, and R. V. A. Oliemans, "Propagation of long waves of finite amplitude at the interface of two viscous liquids," Int. J. Multiphase Flow **11**, 481 (1985).
[20] G. Strang, *Linear Algebra and its Applications* (Harcourt, Brace, and Jovanovich, San Diego, 1988).
[21] H. C. Elman, D. J. Silvester, and A. J. Wathen, *Finite Elements and Fast Iterative Solvers with Applications in Incompressible Fluid Dynamics* (Oxford University Press, Oxford, 2005).
[22] Y. Saad and M. H. Schultz, "GMRES: A generalized minimal residual algorithm for solving nonsymmetric linear systems," SIAM (Soc. Ind. Appl. Math.) J. Sci. Stat. Comput. **7**, 856 (1986).
[23] H. A. van der Vorst and C. Vuik, "The superlinear convergence behaviour of GMRES," J. Comput. Appl. Math. **48**, 327 (1993).
[24] E. F. Kaasschieter, "Preconditioned conjugate gradients for solving singular systems," J. Comput. Appl. Math. **24**, 256 (1988).
[25] H. H. Hu, T. S. Lundgren, and D. D. Joseph, "Stability of core-annular flow with a small viscosity ratio," Phys. Fluids A **2**, 1945 (1990).
[26] M. Kang, H. Shim, and S. Osher, "Level set based simulations of two-phase oil-water flows in pipes," J. Sci. Comput. **31**, 153 (2006).